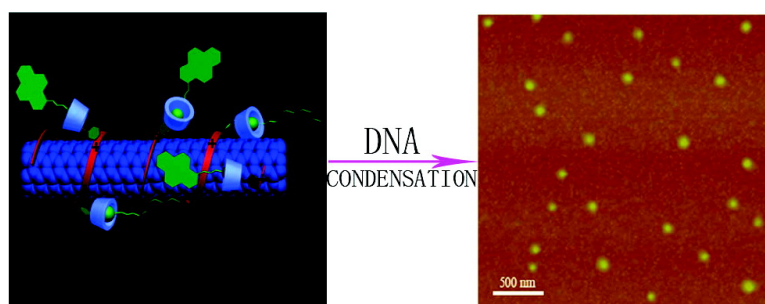


## Supramolecular Architectures of #-Cyclodextrin-Modified Chitosan and Pyrene Derivatives Mediated by Carbon Nanotubes and Their DNA Condensation

Yu Liu, Zhi-Lin Yu, Ying-Ming Zhang, Dong-Sheng Guo, and Yu-Ping Liu

*J. Am. Chem. Soc.*, **2008**, 130 (31), 10431-10439 • DOI: 10.1021/ja802465g • Publication Date (Web): 16 July 2008

Downloaded from <http://pubs.acs.org> on February 8, 2009



### More About This Article

Additional resources and features associated with this article are available within the HTML version:

- Supporting Information
- Access to high resolution figures
- Links to articles and content related to this article
- Copyright permission to reproduce figures and/or text from this article

[View the Full Text HTML](#)

## Supramolecular Architectures of $\beta$ -Cyclodextrin-Modified Chitosan and Pyrene Derivatives Mediated by Carbon Nanotubes and Their DNA Condensation

Yu Liu,<sup>\*,†</sup> Zhi-Lin Yu,<sup>†</sup> Ying-Ming Zhang,<sup>†</sup> Dong-Sheng Guo,<sup>†</sup> and Yu-Ping Liu<sup>‡</sup>

Department of Chemistry, State Key Laboratory of Elemento-Organic Chemistry, and Research Center for Analytical Sciences, Nankai University, Tianjin 300071, P. R. China

Received April 4, 2008; E-mail: yuliu@nankai.edu.cn

**Abstract:**  $\beta$ -Cyclodextrin-modified chitosan **1** was synthesized via the Schiff base reaction between 6-O-(4-formylphenyl)- $\beta$ -cyclodextrin and chitosan (CHIT), and then the supramolecular dyad assemblies **2** and **3** were respectively fabricated from the subunit **1** through the inclusion of adamantane-modified pyrene into the  $\beta$ -cyclodextrin cavity and the wrapping of a CHIT chain on multiwalled carbon nanotubes (MWCNTs). The water-soluble dyad **3** further interacted with adamantane-modified pyrene, forming a stable triad assembly **4**. They were extensively characterized by NMR, thermogravimetric analysis, UV-vis, Raman spectroscopy, X-ray photoelectron spectroscopy, transmission electron microscopy, and atomic force microscopy (AFM). Furthermore, the DNA condensation abilities of **1–4** were validated by AFM and dynamic light scattering, which indicates that the DNA-condensing capability of CHIT can be pronouncedly improved by either the pyrene grafts or the MWCNT medium. The cooperation between cationic and aromatic groups as well as the dispersion of CHIT agglomerates by MWCNTs are the key factors to enhance DNA condensation of cationic polymers.

### Introduction

Gene therapy is a potential method to treat certain disorders by replacing or altering the defective genes with normal ones, especially those caused by genetic anomalies or deficiencies,<sup>1</sup> which has been effectively used in clinical trials.<sup>2</sup> With this objective, DNA condensation is the essential precondition to transport a therapeutic gene to its target position.<sup>3</sup> Schlepping with negative charges and grooves on its main chain,<sup>4</sup> DNA always interacts with substrates possessing positive charges or highly  $\pi$ -conjugated groups, which are implanted to both the major and minor grooves of DNA.<sup>5</sup> Significantly, DNA can be condensed by cationic polymers with an optimal charge ratio (N/P)<sup>6</sup> and appropriate rigidity through noncovalent interactions. As a result, suitable cationic polymers, such as polyamines, PEG-based blocks, and graft copolymers, have been extensively

employed in DNA condensation and gene delivery as vectors.<sup>7</sup> The gene-delivery vectors include viral and nonviral vectors. The nonviral gene-delivery techniques allow for a wide range of products, flexibility of applications, ease of use, low cost of production, and enhanced “genomic” safety as it is relatively nonimmunogenic and will not induce any significant ocular tissue inflammatory responses.<sup>8</sup> Among the nonviral vectors, chitosan (CHIT) has been considered to be a good gene carrier candidate, since it is well-known as an accustomed material with a highly cationic density.<sup>9</sup> Furthermore, modified CHITs with various functional groups have also been widely investigated as they can efficaciously solve problems confronted in DNA condensation,<sup>10</sup> such as preventing the complex of cationic polymer/DNA from dissociating with blood components.

On the other hand, cyclodextrins (CDs), a class of cyclic oligosaccharides with 6–8 D-glucose units, have been extensively investigated in host–guest chemistry for construction of versatile supramolecular aggregations owing to their special

<sup>†</sup> Department of Chemistry, State Key Laboratory of Elemento-Organic Chemistry.

<sup>‡</sup> Research Center for Analytical Sciences.

(1) Ferber, D. *Science* **2001**, *294*, 1638–1642.

(2) (a) Wassarman, P. M. *Cell* **1999**, *96*, 175–183. (b) Yang, X.; Nakao, Y.; Pater, M. M.; Tang, S.-C.; Pater, A. *J. Cell. Biochem.* **1997**, *66*, 309–321.

(3) Hamley, I. W.; Castelletto, V. *Angew. Chem., Int. Ed.* **2007**, *46*, 4442–4455.

(4) Harreis, H. H.; Kornyshev, A. A.; Likos, C. N.; Lowen, H. J.; Sutmann, G. *Phys. Rev. Lett.* **2002**, *89*, 018303–018304.

(5) Kornyshev, A. A.; Leikin, S. *Phys. Rev. Lett.* **1999**, *82*, 4138–4141.

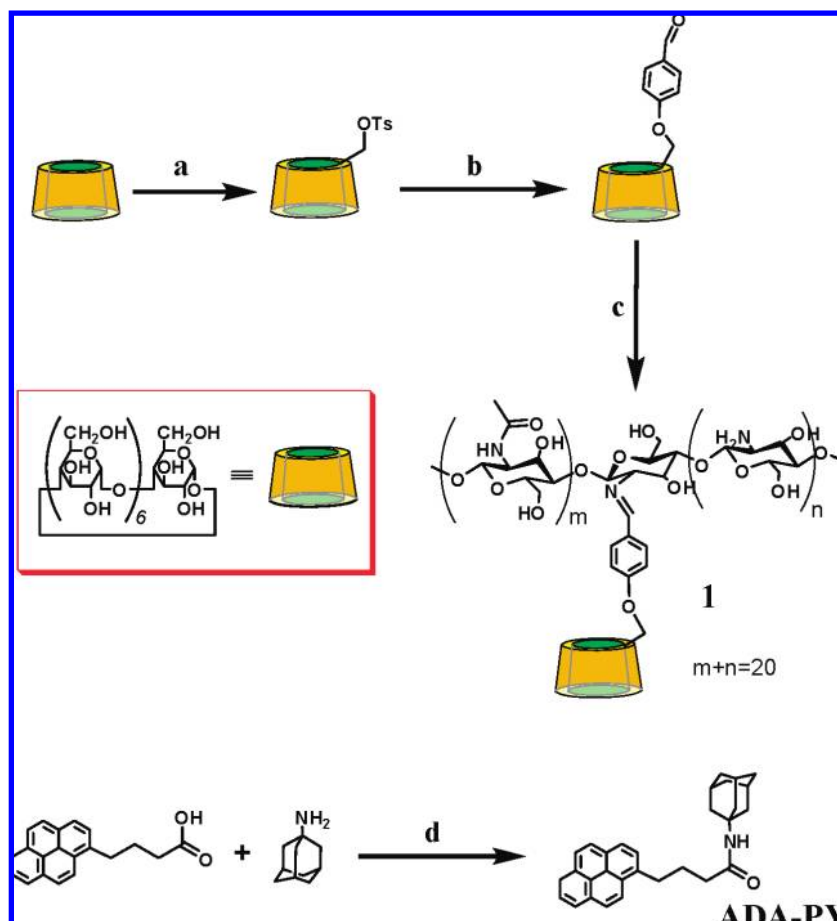
(6) Kima, T.-H.; Jianga, H.-L.; Jerea, D.; Parka, I.-K.; Chob, M.-H.; Nahc, J.-W.; Choia, Y.-J.; Akaiked, T.; Choa, C.-S. *Prog. Polym. Sci.* **2007**, *32*, 726–753.

(7) Nguyen, H. K.; Lemieux, P.; Vinogradov, S. V.; Gebhart, C. L.; GuQrin, N.; Paradis, G.; Bronich, T. K.; Alakhov, V. Y.; Kabanov, A. V. *Gene Ther.* **2000**, *7*, 126–138.

(8) Poon, Y. F.; Zhu, Y. B.; Shen, J. Y.; Chan-Park, M. B.; Choon, N. S. *Adv. Funct. Mater.* **2007**, *17*, 2139–2150.

(9) (a) Felgner, P. L.; Gadek, T. R.; Holm, M.; Roman, R.; Chan, H. W.; Northrop, J. P.; Ringold, G. M.; Danielsen, M. *Proc. Natl. Acad. Sci. U.S.A.* **1987**, *84*, 7413–7417. (b) Boussif, O.; Lezoualch, F.; Zanta, M. A.; Mergny, M. D.; Scherman, D.; Demeneix, B.; Behr, J. P. *Proc. Natl. Acad. Sci. U.S.A.* **1995**, *92*, 7297–7301. (c) Lavertu, M.; Method, S.; TranKhanh, N.; Buschmann, M. D. *Biomaterials* **2006**, *7*, 4815–4824.

(10) Ravi Kumar, M. N. V.; Muzzarelli, R. A. A.; Muzzarelli, C.; Sashiwa, H.; Domb, A. J. *Chem. Rev.* **2004**, *104*, 6017–6084.

Scheme 1. Synthetic Routes of  $\beta$ -CD-Modified CHIT 1 and ADA-PY<sup>a</sup>

<sup>a</sup> Reagents: (a) *p*-Toluene sulfonyl chloride, NaOH/H<sub>2</sub>O; (b) 4-hydroxybenzaldehyde, K<sub>2</sub>CO<sub>3</sub>, dry DMF; (c) CHIT, aqueous CH<sub>3</sub>CO<sub>2</sub>H/MeOH (pH 5); (d) DCC, HOBT, CH<sub>2</sub>Cl<sub>2</sub>.

hydrophobic cavities<sup>11</sup> and also are promising in applications in biological systems.<sup>12</sup> Recently, DNA condensation based on assemblies of  $\beta$ -CD has received considerable attention.<sup>13</sup> Li et al. reported cationic polyrotaxanes constructed by oligoethylenimine-grafted  $\beta$ -CD with a PEO-PPO block polymer, showing the flexible applications as effective polymeric gene-delivery carriers.<sup>13a</sup> In a preliminary research, we found that  $\beta$ -CD-based polypseudorotaxanes with anthryl grafts can act as promising DNA concentrators.<sup>13b</sup> These findings have led us to explore the design and construction of supramolecular architectures based on CD and CHIT to extend the application of nonviral CHIT in DNA condensation and therefore in gene therapy, which has not been reported to the best of our knowledge.

In the present investigation, we report the construction of three supramolecular aggregations based on  $\beta$ -CD-modified CHIT **1** (Scheme 1), including the CHIT-PY dyad **2** (PY represents pyrene), the CHIT-MWCNT dyad **3** (MWCNT represents multiwalled carbon nanotubes), and the CHIT-PY-MWCNT triad **4** as illustrated in Scheme 2. Their applications in DNA

condensation were further investigated in detail. Upon inclusion of  $\beta$ -CD with adamantane-modified pyrene (ADA-PY), the cooperation between cationic and aromatic groups extraordinarily improves the DNA-condensing efficiency of CHIT. Significantly, the homogeneous aqueous solutions of dyad **3** and triad **4** have been shown as stable for more than 1 month, and the employed MWCNTs as the medium also play a crucial role in DNA condensation, which will serve us to further comprehend the application of MWCNTs in the biological field.

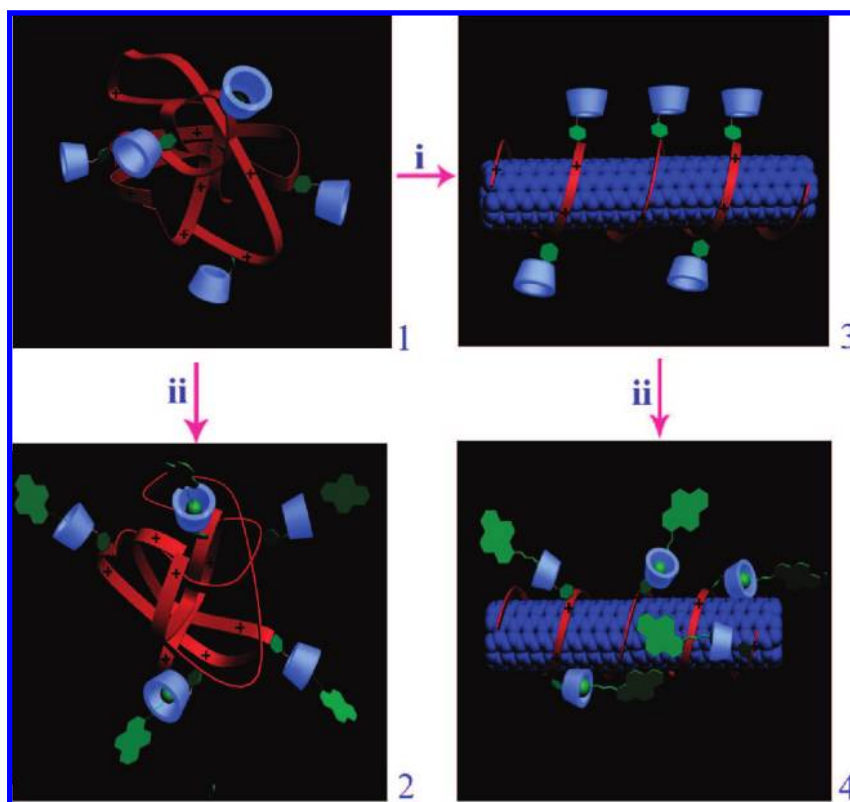
## Results and Discussion

**Preparation and Characterization of 1–4.** The subunit **1** and its supramolecular assemblies **2–4** with MWCNTs and ADA-PY were prepared according to the synthetic routes shown in Schemes 1 and 2 and were adequately identified by <sup>1</sup>H NMR, FT-IR, thermogravimetric analysis, X-ray photoelectron spectroscopy (XPS), transmission electron microscopy (TEM), atomic force microscopy (AFM), and Raman spectroscopy (see Experimental Section or Supporting Information) to estimate their proper components and corresponding configurations. The  $\beta$ -CD-modified CHIT **1** was synthesized by forming a Schiff base between 6-*O*-(4-formylphenyl)- $\beta$ -CD and -NH<sub>2</sub> of CHIT. The FT-IR spectrum of **1** (Figure S1) shows the characteristic vibrations at 1651 and 1683 cm<sup>-1</sup>, representing the cis-vibration and trans-vibration of the Schiff base group, which provides the qualitative evidence that  $\beta$ -CDs have been covalently appended on CHIT. From the <sup>1</sup>H NMR data of **1** (Figure S2),

(11) (a) Connors, K. A. *Chem. Rev.* **1997**, *97*, 1325–1357. (b) Douhal, A. *Chem. Rev.* **2004**, *104*, 1955–1976.

(12) Breslow, R.; Dong, S. D. *Chem. Rev.* **1998**, *98*, 1997–2011.

(13) (a) Li, J.; Yang, C.; Li, H.; Wang, X.; Goh, S. H.; Ding, J. L.; Wang, D. Y.; Leong, K. W. *Adv. Mater.* **2006**, *18*, 2969–2974. (b) Liu, Y.; Yu, L.; Chen, Y.; Zhao, Y.-L.; Yang, H. *J. Am. Chem. Soc.* **2007**, *129*, 10656–10657. (c) Ke, C.-F.; Hou, S.; Zhang, H.-Y.; Liu, Y.; Yang, K.; Feng, X.-Z. *Chem. Commun.* **2007**, 3374–3376.

Scheme 2. Preparation Routes of Supramolecular Assemblies 2–4<sup>a</sup>

<sup>a</sup> (i) MWCNT, HCl solution (pH = 2.0), sonicating for 24 h; (ii) ADA-PY in THF/HCl solution (pH = 2.0) (v/v = 1:20), sonicating for 24 h.

we calculated the number of  $\beta$ -CD units modified on CHIT by digital integration of the NMR signals arising from protons of phenyl and glucose or glucosamine. Each  $\beta$ -CD unit matches approximately 22 glucosamine units. According to the molecular weight of CHIT employed herein ( $M_w = 20\,000$ ), the CHIT polymers are composed of about 117 glucosamine units, and therefore, we estimated that there are five  $\beta$ -CDs appended on each chain of CHIT in **1**. Its substituent degree is not high enough because some amido groups on CHIT have been acetylated at the beginning.

Based on the special binding selectivity of  $\beta$ -CD for adamantane (the complex stability constants of  $\beta$ -CD with adamantane derivatives are over  $10^4$ – $10^5$   $M^{-1}$ ),<sup>14</sup> the aromatic pyrene groups were noncovalently grafted into a CHIT scaffold by combining **1** and ADA-PY, forming the CHIT-PY dyad **2** in satisfactory yield. It can also be inferred from the quantitative analysis of the <sup>1</sup>H NMR results that almost all the cavities of  $\beta$ -CDs were filled by adamantane. As can be seen from Figure S3, comparing the signal integration of protons of  $\beta$ -CD with that of adamantane, the numbers of  $\beta$ -CD and ADA-PY should be consistent with each other.

The dyad **3** was prepared by wrapping **1** on an MWCNT in aqueous solution, and the triad **4** was prepared upon inclusion of ADA-PY into a  $\beta$ -CD cavity.  $\beta$ -CD-modified CHIT **1** was added to a suspension of MWCNTs in aqueous solution, and then the solution was sonicated for 1 h at room temperature. Utilizing CHIT as a solubilizer, the aqueous solution changed from colorless to black (Figure 1), implying the solubilization

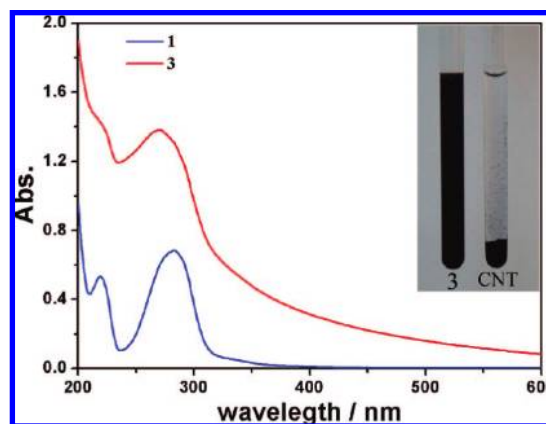


**Figure 1.** UV–vis spectra of **1** and **3**, 1 mg/mL in pH = 4.0 HCl aqueous solution. Inset: Dyad **3** and MWCNT in pH = 4.0 HCl aqueous solution.

of the MWCNTs in aqueous solution. The UV–vis spectrum of dyad **3** presents appreciable absorption in the visible light range, which is ascribed to the diagnostic absorption of MWCNTs. The present result resembles the case of aqueous dispersion of MWCNTs by alginate, which undoubtedly indicates the formation of dyad **3** from enwrapping **1** on the MWCNT. The detailed morphology and component of **3** were further characterized by TEM, AFM, Raman spectroscopy, and XPS. As can be seen from the Raman spectrum of the MWCNT in Figure 2, the D- and G-bands of the MWCNT at ca. 1349 and 1584  $cm^{-1}$ , which are assigned to the defects and in-plane  $E_{2g}$  zone-center mode, were clearly observed for MWCNTs.<sup>16</sup>

(14) (a) Gelb, R. I.; Schwartz, L. M.; Laufer, D. A. *J. Chem. Soc., Perkin Trans. 2* **1984**, 15–21. (b) Harrison, J. C.; Eftink, M. R. *Biopolymers* **1982**, *21*, 1153–1166.

(15) Liu, Y.; Liang, P.; Zhang, H.-Y.; Guo, D.-S. *Small* **2006**, *2*, 874–878.

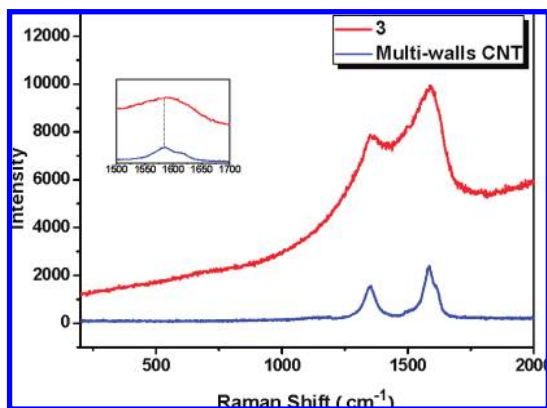


**Figure 2.** Raman spectra (excited with 514.5 nm laser) of dyad **3** (top) and MWCNT (down).

In addition, the D'-band at ca.  $1613\text{ cm}^{-1}$ , which is known to be directly affected by the disorder in MWCNTs, was also observed.<sup>17</sup> For **3**, the D- and G-bands of the MWCNT underwent some minor shifts to a longer wavelength, which appear at  $1351$  and  $1590\text{ cm}^{-1}$ , respectively, in which the upshift of the G-band was more appreciable than that of the D-band. The wrapping of **1** on the surface of the MWCNT changed the elastic constant of **3** compared to pristine MWCNTs.<sup>18</sup> Wrapping **1** on the surface of the MWCNT will cause the field disturbance and the physical strain in the graphite skeleton and then result in the augmentation of the intensity of the D-band. It can be observed that the intensity ratio of D/G-bands of **3** was higher than that of the corresponding MWCNT, which were 0.79 and 0.64, respectively.<sup>19</sup>

XPS represents an effective technique for surface analysis, so we employed the experiments of XPS to give both qualitative and quantitative evidence of dyad **3**. The C1s spectrum of MWCNTs is typically assorted to five components (284.5, 285.5, 286.9, 288.6, 291.4 eV) (Figure 3a).<sup>20</sup> The asymmetric peak at 284.5 eV is contributed by  $\text{sp}^2$ -hybridized graphite-like carbon atoms and carbon atoms bound to hydrogen atoms, which is similar to the graphite showing a high energy region at these sites.<sup>21</sup> The peak at 285.5 eV is due to a defect-containing  $\text{sp}^2$ -hybridized carbon.<sup>22</sup> And also, the peaks at 286.9 and 288.6 eV are depicted, which are due to  $-\text{C}=\text{O}$  and  $-\text{COOH}$ .<sup>23</sup> Finally,  $\text{sp}^2$ -hybridized carbon  $\pi^* \leftarrow \pi$  shakeup (291.4 eV) is

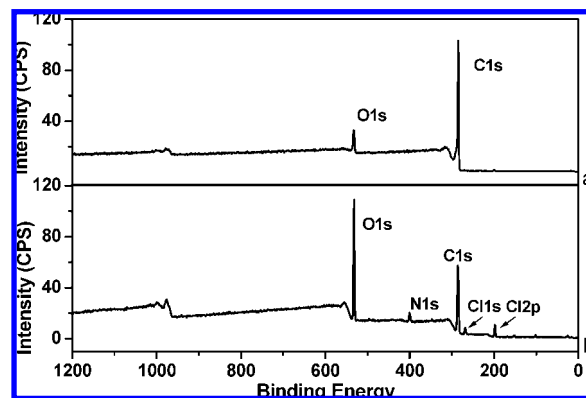


**Figure 3.** XPS survey spectra of MWCNT (a) and dyad **3** (b).

a characteristic peak in the MWCNT.<sup>24</sup> In Figure 3b, all of the expected peaks of associated elements are registered in the XPS survey spectrum of dyad **3**. The nitrogen in the subunit **1** gives the related peak at the  $\sim 400\text{ eV}$ , and the chlorine is introduced by protonation of CHIT with hydrochloric acid. Meanwhile, the C1s spectrum of **3** consists of four components (284.6, 286.3, 288.1, 289.3 eV). Besides the peak at 284.6 eV contributed by a graphite-like carbon, those at 286.3, 288.1, and 289.3 eV are respectively assigned to  $-\text{C}=\text{O}$  (including  $-\text{C}=\text{N}-$  and  $-\text{C}-\text{NH}_2$ ),  $-\text{CO}-\text{NH}-$ , and  $-\text{COOH}$ .<sup>25</sup> Comparing the intensity of the C1s spectrum of dyad **3** to that of the MWCNT, the content of  $-\text{C}=\text{O}$  (286.3 eV) increases remarkably in **3** with the introduction of **1** (Figure S5a). The appearances of  $-\text{C}=\text{N}-$  (286.3 eV) and  $-\text{CO}-\text{NH}-$  (288.1 eV) also indirectly prove the formation of the hybrid between **1** and the MWCNT. Significantly, the disappearance of the  $\pi^* \leftarrow \pi$  shakeup (291.4 eV) demonstrates evidently the wrapping of **1** on the surface of the MWCNT, as the overcast of **1** on the MWCNT exerts appreciable influence over the chemical environment of the MWCNT surface.<sup>26</sup> On the other hand, the N1s spectrum of **3** consists of two components (399.2 and 401.6 eV), in which the peak at 399.2 eV is assigned to  $-\text{C}-\text{NH}_2$  and the peak at 401.6 eV is assigned to  $-\text{CO}-\text{NH}-$ ,  $-\text{NH}_3^+$ , and  $-\text{C}=\text{N}-$ .<sup>27</sup> Moreover, the content ratio of the two kinds of nitrogen is in accordance with the result of  $^1\text{H}$  NMR of **1** (Figure S5b). The ratio of the amount of nitrogen and carbon

- (16) (a) Rao, A. M.; Richter, E.; Bandow, S.; Chase, B.; Eklund, P. C.; Williams, K. A.; Fang, S.; Subaswamy, K. R.; Menon, M.; Thess, A.; Smalley, R. E.; Dresselhaus, G.; Dresselhaus, M. S. *Science* **1997**, *275*, 187–191. (b) Bahr, J. L.; Yang, J.; Kosynkin, D. V.; Bronikowski, M. J.; Smalley, R. E.; Tour, J. M. *J. Am. Chem. Soc.* **2001**, *123*, 6536–6542. (c) Ritter, U.; Scharff, P.; Siegmund, C.; Dmytrenko, O. P.; Kulish, N. P.; Prylutskyy, Y. I.; Belyi, N. M.; Gubanov, V. A.; Komarova, L. I.; Lizunova, S. V.; Poroshin, V. G.; Shlapatskaya, V. V.; Bernas, H. *Carbon* **2004**, *2694*–2700.
- (17) Gao, C.; Jin, Y. Z.; Kong, H.; Whitby, R. L. D.; Acquah, S. F. A.; Chen, G. Y.; Qian, H.; Hartschuh, A.; Silva, S. R. P.; Henley, S.; Fearon, P.; Kroto, H. W.; Walton, D. R. M. *J. Phys. Chem. B* **2005**, *109*, 11925–11932.
- (18) (a) Brown, S. D. M.; Jorio, A.; Dresselhaus, M. S.; Dresselhaus, G. *Phys. Rev. B* **2001**, *64*, 073403–073408. (b) Dyke, C. A.; Tour, J. M. *Nano Lett.* **2003**, *3*, 1215–1218.
- (19) (a) Sinani, V. A.; Gheith, M. K.; Yaroslavov, A. A.; Rakhnyanskaya, A. A.; Sun, K.; Mamedov, A. A.; Wicksted, J. P.; Kotov, N. A. *J. Am. Chem. Soc.* **2005**, *127*, 3463–3472. (b) Caruso, F. *Adv. Mater.* **2001**, *13*, 11–22.
- (20) Beamson, G.; Briggs, D. *High-Resolution XPS of Organic Polymers*; Ellis Harwood: Chichester, 1992.
- (21) van Attekum, P. M. Th. M.; Wetheim; G. K. *Phys. Rev. Lett.* **1979**, *43*, 1896–1898.

- (22) (a) Chattopadhyay, J.; de Jesus Cortez, F.; Chakraborty, S.; Slater, N. K. H.; Billups, W. E. *Chem. Mater.* **2006**, *18*, 5864–5868. (b) Ago, H.; Kugler, T.; Cacialli, F.; Salaneck, W. R.; Shaffer, M. S. P.; Windle, A. H.; Friend, R. H. *J. Phys. Chem. B* **1999**, *103*, 8116–8121.
- (23) (a) Hamon, M. A.; Hu, H.; Bhowmik, P.; Niyogi, S.; Zhao, B.; Itkis, M. E.; Haddon, R. C. *Chem. Phys. Lett.* **2001**, *347*, 8–12. (b) Mawhinney, D. B.; Naumenko, V.; Kuznetsova, A.; Yates, J. T.; Liu, J.; Smalley, R. E. *Chem. Phys. Lett.* **2000**, *324*, 213–216.
- (24) (a) Urszula, D. W.; Viera, S.; Ralf, G.; Sung, H. J.; Byung, H. K.; Hyun, J. L.; Lothar, L.; Yung, W. P.; Savas, B.; David, T.; Siegmars, R. *J. Am. Chem. Soc.* **2005**, *127*, 5125–5131. (b) Lee, W. H.; Kim, S. J.; Lee, W. J.; Lee, J. G.; Haddon, R. C.; Reucroft, P. J. *Appl. Surf. Sci.* **2001**, *181*, 121–127.
- (25) (a) Peng, H. Q.; Alemany, L. B.; Margrave, J. L.; Khabashesku, V. N. *J. Am. Chem. Soc.* **2003**, *125*, 15174–15182. (b) Urszula, D. W.; Viera, S.; Ralf, G.; Sung, H. J.; Byung, H. K.; Hyun, J. L.; Lothar, L.; Yung, W. P.; Savas, B.; David, T.; Siegmars, R. *J. Am. Chem. Soc.* **2005**, *127*, 5125–5131.
- (26) (a) Yang, D.-Q.; Rochette, J.-F.; Sacher, E. *Langmuir* **2005**, *21*, 8539–8545. (b) Yang, D.-Q.; Sacher, E. *Surf. Sci.* **2002**, *504*, 125–137. (c) Yang, D.-Q.; Sacher, E. *Surf. Sci.* **2003**, *516*, 45–55.
- (27) (a) Khan, M. M. T.; Srivastava, S. *Polyhedron* **1988**, *7*, 1063–1068. (b) Chan, H. S. O.; Hor, T. S. A.; Sim, M. M.; Tan, K. L.; Tan, B. T. G. *Polym. J.* **1990**, *22*, 883–892. (c) Dash, K. C.; Folkesson, B.; Larsson, R.; Mohapatra, M. *J. Electron Spectrosc.* **1989**, *49*, 343–352.

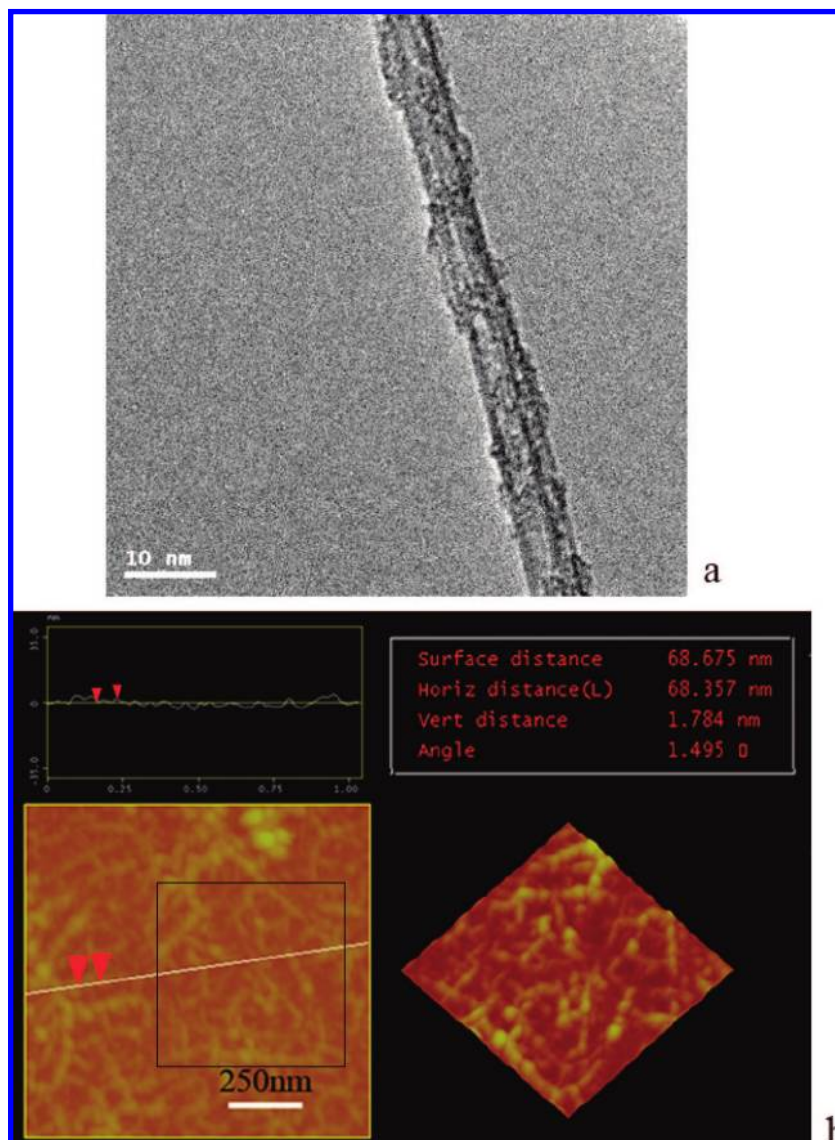


**Figure 4.** TEM graph (a) and AFM image (b) of **3**.

in **3** is 8.6%, which reflects the degree of overcast of **1** on the MWCNT to some extent.<sup>28</sup>

The morphology of dyad **3** was observed by TEM and AFM. As can be seen from Figure 4a, there are clearly belt-like substances wrapped on the MWCNT, in which the belt represents the  $\beta$ -CD-modified CHIT **1**. Moreover, the AFM image of dyad **3** has also clearly showed that there are many beads with a height of  $\sim 1.5$  nm on the surface of the MWCNT (Figure 4b). These beads are reasonably considered to be  $\beta$ -CD units according to the size/shape of  $\beta$ -CD. The results obtained by both TEM and AFM measurements illustrated that  $\beta$ -CD-modified CHIT **1** orderly wrapped on the surface of the MWCNT with the farthest dispersion, forming supramolecular dyad **3**.

The triad **4** was obtained by addition of ADA-PY in the aqueous solution of **3** following the same method as to prepare dyad **2**. It is observed from  $^1\text{H}$  NMR spectrum (Figure S4) that almost all the cavities of  $\beta$ -CDs are filled by adamantane. In

addition, the homogeneous black solutions of **3** and **4** have been shown as stable for more than 1 month, which promises further applications in condensation of calf thymus DNA. The employment of both the pyrene group and MWCNT provides beneficial insight to DNA condensation based on CHIT polymers.

**DNA Condensations of 1–4.** Although there have been some reports on the  $\beta$ -CD-modified CHIT,<sup>29</sup> the DNA condensation behavior has never been investigated previously. The experiment of DNA condensation by **1** was first performed in pH = 4.0 solution and identified by the comparison of the AFM images of calf thymus DNA in the absence and presence of **1**. As shown in Figure 5a, the AFM image of the intact DNA presents the configuration of dispersive chains. When **1** was used to agglomerate calf thymus DNA that was purified as previously reported until UV absorbance 260 nm/280 nm was  $> 1.9$  using

(28) Holzinger, M.; Abraham, J.; Whelan, P.; Graupner, R.; Ley, L.; Hennrich, F.; Kappes, M.; Hirsch, A. *J. Am. Chem. Soc.* **2003**, *125*, 8566–8580.

(29) (a) Auzely-Velty, R.; Rinaudo, M. *Macromolecules* **2001**, *34*, 3574–3580. (b) Ravoo, B. J.; Jacquier, J.-C.; Wenz, G. *Angew. Chem., Int. Ed.* **2003**, *42*, 2066–2070. (c) Van der Heyden, A.; Wilczewski, M.; Labbe, P.; Auzely, R. *Chem. Commun.* **2006**, 3220–3222.

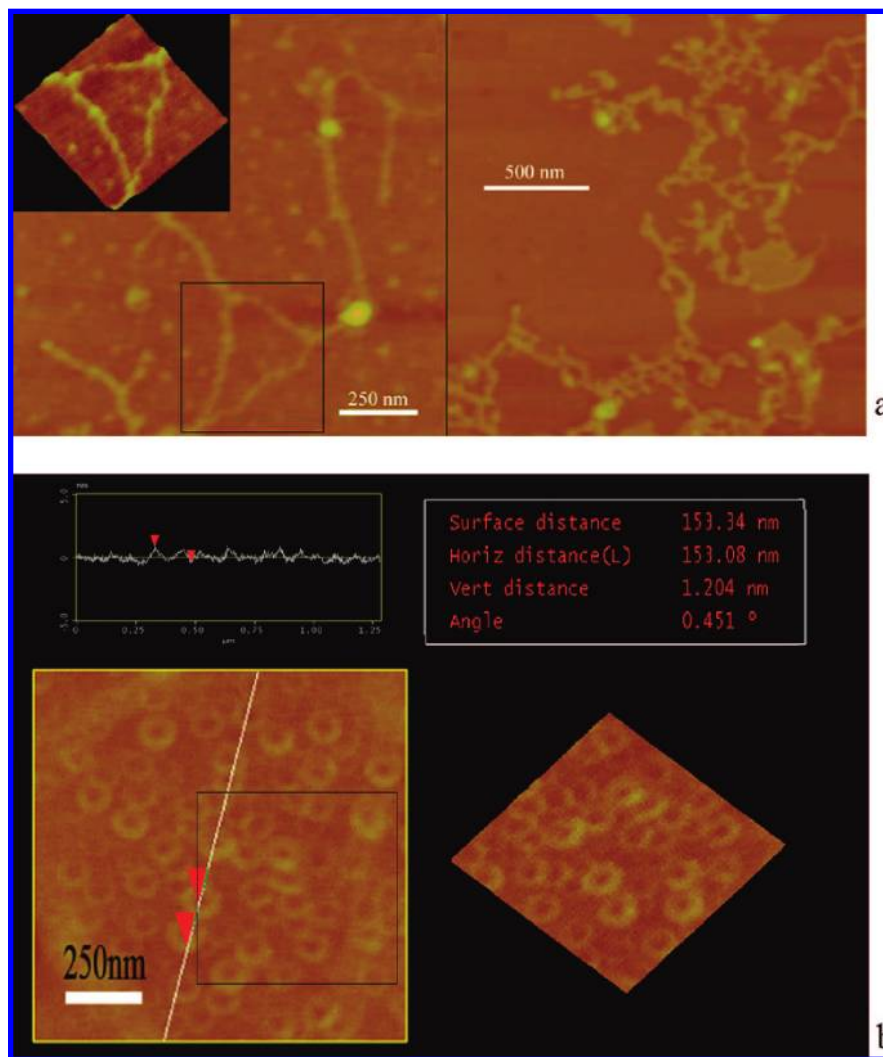


**Figure 5.** AFM images of calf thymus DNA (2 ng/ $\mu$ L) in pH = 4.0 HCl solution (a) in absence of and (b) in presence of **1** (2 ng/ $\mu$ L).

phenol,<sup>30</sup> it was found that the free DNA chains were condensed to uniform hollow loops (Figure 5b). The phenomenon from AFM images in Figure 5 adequately illuminates the moderate DNA-condensing capability of **1**. The present result is in accordance with that of pristine CHIT that can induce the condensation of calf thymus DNA, but the efficiency is not high enough.<sup>31</sup>

Highly  $\pi$ -conjugated groups, such as anthracene, perylene, and pyrene, can also interact with DNA to penetrate into its grooves besides the positive cations.<sup>32</sup> Therefore, CHIT derivatives appended with some aromatic groups may dramatically improve CHIT's efficiency of DNA condensation via the synergistic interactions between cations and aromatic groups. As the  $\beta$ -CD unit in **1** prefers to accommodate the adamantane portion into its cavity other than the pyrene portion, the conformation of dyad **2** with exposed pyrene grafts (shown in Scheme 2) provides a suitable preorganizational structure to cooperatively induce DNA condensation. The experiment of dyad **2** condensing DNA was performed as well as that of **1**. The dyad **2** was much more effective in condensing calf thymus

DNA than the subunit **1**. As can be seen from the AFM image of calf thymus DNA upon addition of dyad **2** (Figure 6), the free calf thymus DNA chains were condensed to infarctate particles by dyad **2** rather than the hollow loops by **1**. In addition, the improved condensing capability of **2** is also reflected by the size of DNA condensate. The DNA condensates induced by **2** are about 200 nm wide in the average diameter. The pronounced enhancement of DNA condensing efficiency from **1** to **2** is obviously ascribed to the cooperative aromatic pyrenes besides the inherent  $-\text{NH}_3^+$  cations on CHIT. For gene therapy in clinical trials, which transfect DNA into a cell by membrane endocytosis, shrunk DNA would be favorable to enter a cell for genetic expression. The excellent DNA condensation of dyad **2** provides a novel route to extend effectively the application of CHIT in the biochemistry field from the standpoint of supramolecular cooperativity.

On the other hand, the relatively poor DNA-condensing capability of CHIT may originate from the preferable agglomer-

(30) Maniatis, T.; Fritsch, E. F.; Sambrook, J. *Molecular Cloning A Laboratory Manual*; Cold Spring Harbor Laboratory: New York, 1982.  
 (31) Danielsen, S.; Vårum, K. M.; Stokke, B. T. *Biomacromolecules* **2004**, *5*, 928–936.

(32) (a) Ikeda, T.; Yoshida, K.; Schneider, H.-J. *J. Am. Chem. Soc.* **1995**, *117*, 1453–1454. (b) Mayer-Enthart, E.; Wagenknecht, H.-A. *Angew. Chem., Int. Ed.* **2006**, *45*, 3372–3375. (c) Wegner, S. V.; Okesli, A.; Chen, P.; He, C. *J. Am. Chem. Soc.* **2007**, *129*, 3474–3475.

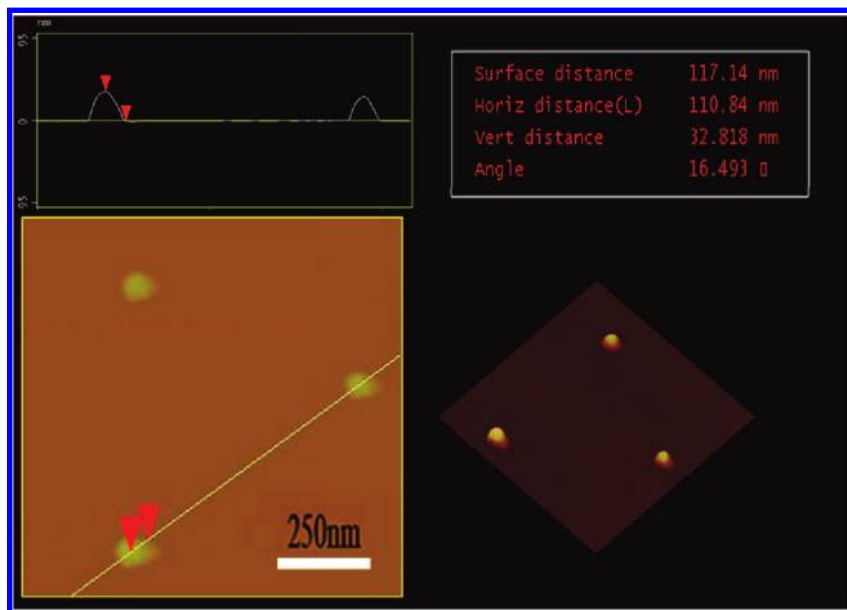


**Figure 6.** AFM image of calf thymus DNA (2 ng/ $\mu$ L) in pH = 4.0 HCl solution in presence of **2** (2 ng/ $\mu$ L).

ate character of most polymers.<sup>33</sup> It is reasonably accepted that the agglomerate conformation of CHIT makes the positive cations shielded in the coil to some extent and, therefore, restrains the percent of  $-\text{NH}_3^+$  groups available to interact with DNA. Dramatically, the dyad **3** mediated by MWCNTs also provides considerable DNA-condensing effects as compared with **1** in the same experimental conditions. When the dyad **3** was employed in DNA condensation, the calf thymus DNA chains were induced to condense as compact particles, with an average diameter of 80 nm (Figure 7a), but not loose loops. This observation implies that MWCNTs should play a great role in DNA condensation. In earlier reports, chitosan as a soft material can wrap MWCNTs to increase the solubility of MWCNTs in aqueous solution.<sup>34</sup> In the meantime, the disadvantageous agglomerate configuration of CHIT was overcome by interacting with MWCNTs to arrange themselves on the surface of MWCNTs as highly dispersed polymers. Hence, more active  $-\text{NH}_3^+$  cations can interact with DNA grooves, and the MWCNT-mediated dyad **3** exhibits much more effective DNA condensation than the corresponding **1**. This interpretation can be enforced by the aforementioned AFM and TEM images of dyad **3** (Figure 4) where **1** is orderly wrapped on the surface of the MWCNT with the farthest dispersion.

Inspired by the improved effects of DNA condensation of dyads **2** and **3**, the CHIT-PY-MWCNT triad **4** was further investigated as a combinatorial vector. An AFM image of calf thymus DNA in the presence of triad **4** shows that DNA exists as compact particles with an average diameter of 160 nm (Figure 7b). Compared with dyad **3**, the introduction of functional pyrene groups in triad **4** obviously promotes DNA condensation (the DNA particles enlarged from 80 nm wide by **3** to 160 nm wide by **4**). This fact implies that pyrenes can further increase the DNA-condensing capability of CHIT mediated by MWCNT. However, the efficiency of DNA condensation of triad **4** is not

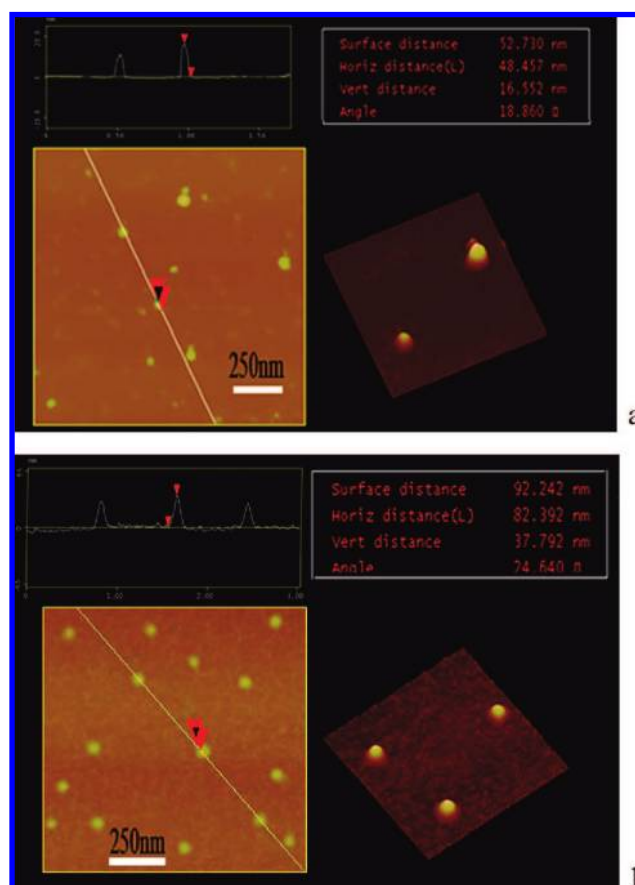


**Figure 7.** AFM images of calf thymus DNA (2 ng/ $\mu$ L) in pH = 4.0 HCl solution in the presence of (a) **3** (4 ng/ $\mu$ L) and (b) **4** (4 ng/ $\mu$ L).

superior to that of dyad **2**. The comparison between **2** and **4** indicates that pyrenes possibly can also destroy the agglomerate of CHIT to some extent besides interacting with DNA. On the other hand, pyrene could attach to MWCNTs through  $\pi$ -stacking interactions,<sup>35</sup> which may decrease the activity of pyrene condensing DNA. Although the final triad **4** does not provide the highest efficiency with respect to DNA condensation, the

(33) Philippova, O. E.; Volkov, E. V.; Sitnikova, N. L.; Khokhlov, A. R. *Biomacromolecules* **2001**, *2*, 483–490.

(34) (a) Moore, V. C.; Strano, M. S.; Haroz, E. H.; Hauge, R. H.; Smalley, R. E. *Nano Lett.* **2003**, *3*, 1379–1382. (b) Zhang, M. G.; Gorski, W. *J. Am. Chem. Soc.* **2005**, *127*, 2058–2059. (c) Luo, X. L.; Xu, J. J.; Wang, J. L.; Chen, H. Y. *Chem. Commun.* **2005**, 2169–2171.



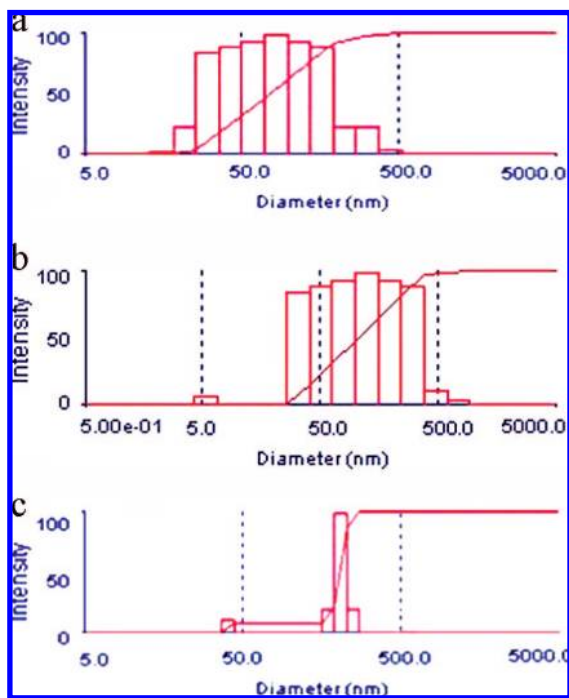


**Figure 8.** Hydrodynamic diameter distributions  $f(D_h)$  of DNA particles condensed by (a) **1**, (b) **3**, and (c) **4** at a scattering angle of  $90^\circ$  at  $25^\circ\text{C}$ . In the measurements, the DNA concentration is  $2\text{ ng}/\mu\text{L}$ , and the concentrations of compactors are 2, 4, and  $4\text{ ng}/\mu\text{L}$  for **1**, **3**, and **4**, respectively.

MWCNT has been used as a carrier to deliver genes and peptides across cell membranes<sup>36</sup> as well as an intravenous abluent and for cancer therapy,<sup>37</sup> and therefore the species mediated by MWCNTs can be potentially used for gene or drug delivery thanks to its ability of carrying MWCNTs.

**Size Distribution of DNA Particles.** From DLS measurements at a scattering angle of  $90^\circ$ , the hydrodynamic diameters of the DNA particles condensed by **1**, **3**, and **4** are about  $68 \pm 0.02$ ,  $114 \pm 0.21$ , and  $157 \pm 0.06\text{ nm}$ , respectively (Figure 8). The sizes are not in accordance with those observed on AFM images. This can be attributed to the difference in hydrodynamic diameter of particles in aqueous solution compared to the diameter of particles in the dry state observed in AFM. However, the sizes of the DNA particles are in the same order of  $1 < 3 < 4$  as those measured by AFM, which also demonstrates that the DNA-condensing capabilities of dyad **3** and triad **4** are much more efficacious than that of **1** owing to the employments of MWCNTs as a dispersing medium of CHIT and pyrene as a synergistic DNA intercalator. Meanwhile, the hydrodynamic diameter distribution  $f(D_h)$  of DNA particles condensed by **4** is more concentrative than the other two condensed by **1** and **3**,

which also indicates that the triad **4** possesses a more effective capability of DNA condensation.

## Conclusion

In summary, three supramolecular assemblies **2–4** were constructed based on  $\beta$ -CD-modified CHIT **1**. Owing to the high binding ability and selectivity of  $\beta$ -CDs for adamantane, the dyad **2** and triad **4** were obtained in good yield with sufficient pyrene groups noncovalently grafted. Wrapping **1** on an MWCNT makes the MWCNT moderately water-soluble, and the homogeneous black solutions of **3** and **4** have been shown to be as stable for more than 1 month. Moreover, the CHIT chain in **3** and **4** is more dispersive than the subunit **1** on the surface of the MWCNT. In DNA-condensing experiments, CHIT appended with pyrene groups or mediated by MWCNTs provides much more effective DNA condensation than CHIT itself. Pyrene can supply the binding site to implant into the grooves of DNA, in addition to the inherent cations of CHIT. MWCNTs can induce the dispersion of CHIT agglomerates, which makes the cationic polymer more suitable to interaction with DNA. The results obtained explore two novel ways based on the supramolecular concepts to enhance the DNA-condensing efficiency of cationic polymers, which is of significance for the potential applications of supramolecular architectures in DNA chemistry to control gene expression and delivery.

## Experimental Section

**Materials.** Chitosan (CHIT) was purchased from Qingdao Brightmoon Seaweed Industry Co., Ltd., and used without any purification.  $\beta$ -Cyclodextrin ( $\beta$ -CD) of reagent grade (Shanghai Reagent Factory) was recrystallized twice from water and dried under vacuum at  $95^\circ\text{C}$  for 24 h prior to use. Multiwalled carbon nanotubes (MWCNT, purity  $>95\%$ , diameter within  $5\text{--}10\text{ nm}$ ) produced by chemical vapor deposition (CVD) was obtained from Shenzhen Nanotech. Port. Co. Ltd., China, and was purified according to the reported procedures.<sup>38</sup> The commercially available calf thymus DNA was purified until UV absorbance  $260\text{ nm}/280\text{ nm}$  was  $>1.9$  using phenol. The DNA concentration per nucleotide was determined by absorption spectroscopy using the molar absorption coefficient ( $\epsilon = 6600\text{ mol}^{-1}\text{ m}^3\text{ cm}^{-1}$ ) at  $260\text{ nm}$ .<sup>30</sup> All of the DNA condensation were carried out in  $\text{pH} = 4.0$  HCl aqueous solution under the given mass ratio between DNA and compactor.

**Instruments.** FT-IR spectrum was obtained with a BRUKER TENSOR 27 instrument. The sample was prepared as pellets using spectroscopic grade KBr. UV-vis spectra were recorded in a conventional quartz cell (light path  $10\text{ mm}$ ) on a Shimadzu UV-2401PC spectrophotometer equipped with a PTC-348WI temperature controller to keep the temperature at  $25^\circ\text{C}$ .  $^1\text{H}$  NMR spectra were recorded in a  $\text{D}_2\text{O}$  solution (pD adjusted by DCl) at  $25^\circ\text{C}$  on a Varain Mercury Plus 400. The thermogravimetric analysis was recorded with a RIGAKU Standard type with a heating rate of  $10^\circ\text{C}/\text{min}$  from room temperature to  $800^\circ\text{C}$ . Raman spectra were recorded on Renishaw in-Via Raman Microscope. X-ray photoelectron spectroscopy (XPS) was recorded using a Kratos Axis Ultra DLD spectrometer employing a monochromatic Al K $\alpha$  X-ray source ( $h\nu = 1486.6\text{ eV}$ ), hybrid (magnetic/electrostatic) optics, and a multichannel plate and delay line detector (DLD). All XPS spectra were recorded using an aperture slit width of  $300 \times 700\ \mu\text{m}$ , survey spectra were recorded with a pass energy of  $160\text{ eV}$ , and high resolution spectra were recorded with a pass energy of  $40\text{ eV}$ . Atomic force microscopy (AFM) were performed using a multi-mode IIIa AFM (Veeco Metrology, USA) under ambient conditions,

- (35) (a) Chen, R. J.; Zhang, Y.; Wang, D.; Dai, H. *J. Am. Chem. Soc.* **2001**, *123*, 3838–3839. (b) Besteman, K.; Lee, J.-O.; Wiertz, F. G. M.; Heering, H. A.; Dekker, C. *Nano Lett.* **2003**, *3*, 727–730. (c) Kinsella, J. M.; Ivanisevic, A. *Nat. Nanotechnol.* **2007**, *2*, 596–597.
- (36) Keren, K.; Berman, R. S.; Buchstab, E.; Sivan, U.; Braun, E. *Science* **2003**, *302*, 1380–1382.
- (37) (a) Singh, R.; Pantarotto, D.; Lacerda, L.; Pastorin, G.; Klumpp, C.; Prato, M.; Bianco, A.; Kostarelos, K. *Proc. Natl. Acad. Sci. U.S.A.* **2006**, *103*, 3357–3362. (b) Singh, N.; Pillay, V.; Choonara, Y. E. *Prog. Neurobiol.* **2007**, *81*, 29–44.

- (38) Liu, J.; Rinzler, A. G.; Dai, H.; Hafner, J. H.; Bradley, R. K.; Boul, P. J.; Lu, A.; Iverson, T.; Shelimov, K.; Huffman, C. B.; Rodriguez-Macias, F.; Shon, Y.-S.; Lee, T. R.; Colbert, D. T.; Smalley, R. E. *Science* **1998**, *280*, 1253–1256.

and samples were prepared by dropping the solution on mica. Transmission electron microscopy (TEM) experiments were performed using a Philips Tacnai G<sup>2</sup> 20 S-TWIN microscope operating at 200 kV. For visualization by TEM, samples were prepared by dropping a solution of production on a copper grid. Dynamic light scattering (DLS) measurements were performed on a laser light scattering spectrometer (BI-200SM) equipped with a digital correlator (Turbo Corr.) at 636 nm. All samples were first prepared by filtering solutions (about 1 mL) through a 0.45 mm Millipore filter into a clean scintillation vial and were then characterized at 25 °C.

**Preparation of  $\beta$ -CD-Modified CHIT 1.** CHIT (200 mg) was dissolved in a mixture of 0.2 M aqueous CH<sub>3</sub>CO<sub>2</sub>H (14 mL) and MeOH (10 mL), and a 0.5 M NaOH solution was added dropwise to adjust to pH = 5.0. After added 6-*O*-(4-formylphenyl)- $\beta$ -CD (200 mg),<sup>39</sup> the system was stirred at 60 °C for 24 h under a nitrogen atmosphere and then cooled to room temperature. A 0.5 M NaOH solution was used to precipitate the CHIT compounds. The precipitate was successively washed with water, 1:1 water-EtOH, and EtOH and dried to give **1** (240 mg). IR (KBr, cm<sup>-1</sup>) 3746, 3011, 2884, 1734, 1698, 1683, 1651, 1557, 1506, 1456, 1165, 1066, 833, 729, 465; <sup>1</sup>H NMR (400 MHz, 1 mol/L DCl in D<sub>2</sub>O, ppm)  $\delta$  9.67 (1 H, -CH=N-), 7.82 (2 H, H of phenyl), 7.09 (2 H, H of phenyl), 4.90–5.10 (7 H, C-1 H of  $\beta$ -CD), 3.09 and 3.40–4.10 (169 H, C-2, C-3, C-4, C-5, C-6 H of  $\beta$ -CD and protons of CHIT), 1.98 (27 H, -C=OCH<sub>3</sub> of CHIT).

**Synthesis of Adamantane-Modified Pyrene (ADA-PY).<sup>40</sup>** 1-Pyrenebutyric acid (75.3 mg, 0.26 mmol) activated by 1-hydroxybenzotriazole (HOBT, 35.13 mg, 0.26 mmol) was dissolved in 14 mL of dry dichloromethane (CH<sub>2</sub>Cl<sub>2</sub>) at 0 °C for 0.5 h. 1-Adamantanamine (39.5 mg, 0.26 mmol) and *N,N'*-dicyclohexylcarbodiimide (DCC, 53.6 mg, 0.26 mmol) dissolved in 14 mL of dry CH<sub>2</sub>Cl<sub>2</sub> were added dropwise into the solution mentioned above. The reaction mixture was stirred at 0 °C for 24 h and then allowed to rise to room temperature for 24 h. After removal of insoluble salts by filtration, the filtrate was extracted with water three times (3  $\times$  50 mL), and then the mixture was concentrated and purified by silica gel column chromatography eluting with CH<sub>2</sub>Cl<sub>2</sub> and 1:3 petroleum ether/ethyl acetate (v/v) to yield a white crystalline solid (0.22 g). <sup>1</sup>H NMR (400 MHz, CDCl<sub>3</sub>, TMS, ppm)  $\delta$  7.85, 7.99, 8.13, 8.29 (9 H, H of pyrene), 5.02 (1 H, -NH-C=O), 3.38 (2 H, -CH<sub>2</sub>-C=O of butyl acid), 2.13–2.22 (4 H, -(CH<sub>2</sub>)<sub>4</sub>- of butyl), 2.01–2.07 (3 H, -CH- of adamantane), 1.97 (6 H, -CH<sub>2</sub>- of adamantane), 1.66 (6 H, -CH<sub>2</sub>- of adamantane), MS (ESI): *m/z* 422.54 [M + H]<sup>+</sup>.

**Preparation of Dyad 2. 1** (20 mg) was dissolved in a pH 2.0 HCl solution (20 mL), and a THF solution (1 mL) containing ADA-PY (20 mg) was added under sonication. After sonicating for 24 h, the suspension was centrifuged to remove the insolubles, and then the solvent was removed under vacuum, giving the dyad **2** (16 mg). <sup>1</sup>H NMR (400 MHz, 1 mol/L DCl in D<sub>2</sub>O, ppm)  $\delta$  9.21 (1 H, -CH=N-), 7.43–7.45 (4 H, H of pyrene), 7.35 (2 H, H of phenyl), 6.69 and 7.10 (5 H, H of pyrene), 6.55 (2 H, H of phenyl), 2.50–3.80 (169 H, C-2, C-3, C-4, C-5, C-6 H of  $\beta$ -CD and protons of CHIT), 1.90–2.00, 2.10 (6 H, -CH<sub>2</sub>- of butyl), 1.47–1.50 (3H, -CH- of adamantane), 0.82 (12 H, -CH<sub>2</sub>- of adamantane), 0.58 (27 H, -C=OCH<sub>3</sub> of CHIT).

**Preparation of Dyad 3.** 15 mg of purified MWCNTs were added to the pH 2.0 HCl solution (120 mL) of **1** (60 mg), followed by mild ultrasonication for 1 h. The suspension was centrifuged to remove the insoluble MWCNTs, and the solution was filtered on polytetrafluoroethylene membranes (pore size: 0.22  $\mu$ m), giving dyad **3** (25 mg), which was characterized by the methods of thermogravimetric analysis, UV-vis, Raman and XPS, TEM, and AFM.

**Preparation of Triad 4.** Dyad **3** (10 mg) was similarly treated according to the method of preparation of **2**, giving triad **4** (9 mg). <sup>1</sup>H NMR (400 MHz, 1 mol/L DCl in D<sub>2</sub>O, ppm)  $\delta$  7.79 (1 H, -CH=N-), 7.56–7.58 (4 H, H of pyrene), 7.23 (2 H of pyrene), 7.08–7.10 (3H, H of pyrene), 6.90 (2 H, H of phenyl), 6.70–6.74 (2 H, H of phenyl), 2.20–4.20 (169 H, C-2, C-3, C-4, C-5, C-6 H of  $\beta$ -CD and protons of CHIT), 2.00–2.10 (6 H, -CH<sub>2</sub>- of butyl), 1.58–1.62 (15H, -CH<sub>2</sub>-, -CH- of adamantane), 0.60–1.01 (27 H, -C=OCH<sub>3</sub> of CHIT).

**Acknowledgment.** This work was supported by 973 Program (2006CB932900), NNSFC (20673061 and 20421202), Tianjin Natural Fund (07QTPJC29600), and 111 Project (B06005), which are gratefully acknowledged. We thank the reviewers for their valuable comments and suggestions regarding the revision. We also thank Dr. Steven Brokman at Iowa State University and Dr. Xiaopeng Bai at Helicos BioSciences Corporation for assistance in the preparation of this manuscript.

**Supporting Information Available:** FT-IR of **1**; <sup>1</sup>H NMR of **1**, **2**, and **4**; thermogravimetric analysis of MWCNT, **1**, and **3**; XPS C1s spectra of **3** and MWCNT; XPS N1s spectrum of **3**. This material is available free of charge via the Internet at <http://pubs.acs.org>.

JA802465G

(39) Liu, Y.; Fan, Z.; Zhang, H.-Y.; Yang, Y.-W.; Ding, F.; Liu, S.-X.; Wu, X.; Wada, T.; Inoue, Y. *J. Org. Chem.* **2003**, *68*, 8345–8352.

(40) Katoh, M.; Sodeoka, M. *Bioorg. Med. Chem. Lett.* **1999**, *9*, 881–884.